Available online at www.sciencedirect.com
ScienceDirect
Journal of Sound and Vibration 316 (2008) 248–262
JOURNAL OF SOUND AND VIBRATION
www.elsevier.com/locate/jsvi

Nonlinear dynamic mechanism of vocal tremor from voice analysis and model simulations

Yu Zhang*, Jack J. Jiang

Department of Surgery, Division of Otolaryngology Head and Neck Surgery, University of Wisconsin Medical School, Medical Science Center, Room 5745, 1300 University Avenue, Madison, WI 53792-7375, USA

Received 20 February 2007; received in revised form 11 February 2008; accepted 18 February 2008
Handling Editor: S. Bolton
Available online 2 April 2008

Abstract

Nonlinear dynamic analysis and model simulations are used to study the nonlinear dynamic characteristics of vocal folds with vocal tremor, which can typically be characterized by low-frequency modulation and aperiodicity. Tremor voices from patients with disorders such as paresis, Parkinson's disease, hyperfunction, and adductor spasmodic dysphonia show low-dimensional characteristics, differing from random noise. Correlation dimension analysis statistically distinguishes tremor voices from normal voices. Furthermore, a nonlinear tremor model is proposed to study the vibrations of the vocal folds with vocal tremor. Fractal dimensions and positive Lyapunov exponents demonstrate the evidence of chaos in the tremor model, where amplitude and frequency play important roles in governing vocal fold dynamics. Nonlinear dynamic voice analysis and vocal fold modeling may provide a useful set of tools for understanding the dynamic mechanism of vocal tremor in patients with laryngeal diseases.

1. Introduction

Complex phenomena such as bifurcation and chaos have been widely observed in mechanical vibratory systems [1–3]. In recent years, nonlinear mechanisms of abnormal or disordered behaviors have also been suggested in biomedical systems [4–12]. These investigations examine potential contributions of nonlinear dynamics to the analysis and modeling of physiologic disorders. Tremor denotes involuntary and approximately sinusoidal oscillation in biomedical systems and may cause movement and voice disorders. The oscillatory patterns of tremor in human physical function are caused most directly by the asynchrony of antagonistic muscle groups [8–10]. Biomedical systems inevitably exhibit some natural physiologic tremor, but excessive tremor becomes pathologic when it impairs an individual's ability to perform normal physical behaviors. Unlike movement disorders from limb tremor [11,12], nonlinear dynamic characteristics of voice disorders resulting from vocal tremor have not yet been studied.

*Corresponding author. Tel.: +1 608 265 9854; fax: +1 608 265 2139.
E-mail address: zhang@surgery.wisc.edu (Y. Zhang).

0022-460X/$ - see front matter © 2008 Elsevier Ltd. All rights reserved.
doi:10.1016/j.jsv.2008.02.026

Voice tremor has been pathophysiologically linked to respiratory, laryngeal, and articulatory aspects of phonation. In terms of the laryngeal aspect, slow rhythmic motor unit firings of laryngeal muscles may result in vocal tremors. The clinical signals of vocal tremor are low-frequency modulations of voice frequency or amplitude and intermittent voice instability [13–16]. The typical frequency range for pathological tremor is between 4 and 7 Hz. Recent measures of tremor intensity and frequency have linked vocal tremor to pathological hoarseness [13,16–19]. Voice perturbation analysis has established that tremor voices may display moderately elevated frequency and amplitude perturbations [18]. However, traditional voice methods [15,18,20] cannot be applied to the quantitative analysis of aperiodic or irregular voices observed in vocal tremor to obtain information about the underlying mechanism. Nonlinear dynamic analysis [21] represents a valuable method for describing the complexity of systems and has been applied to describe disordered voices from patients with laryngeal pathologies, including Parkinsonian dysarthria [22], vocal polyps [6,23], and laryngeal paralysis [24]. On the other hand, nonlinear vocal fold models allow simulation of a wide range of phonation phenomena [4,5,25], and have been used to predict information about the dynamics of disordered voices associated with laryngeal pathologies [16,26,27]. Although the importance of nonlinear dynamic methods in analyzing and modeling tremor voices is clear, few studies have been performed to explore the dynamic mechanism of vocal tremor from a nonlinear dynamics point of view.

In this paper, we employ nonlinear dynamic voice analysis as well as vocal fold modeling to study the dynamics of vocal tremor in laryngeal systems with a variety of laryngeal diseases such as paresis, Parkinson's disease, hyperfunction, and adductor spasmodic dysphonia. The statistical difference between normal and tremor voices is examined using nonlinear dynamic analysis. Based on the estimated system variable numbers from correlation dimension analysis, we propose a nonlinear tremor model coupled with a vocal fold system to study the dynamic mechanism of vocal tremor. Lyapunov exponents and Kaplan–Yorke dimensions are calculated. Bifurcation diagrams are used to investigate the effects of tremor amplitude and frequency on vocal fold dynamics. The results reveal the nonlinear dynamic mechanism of vocal tremor in patients with laryngeal pathology.

2. Nonlinear dynamic analysis of pathological voices from patients with vocal tremor

2.1. Database

The voice samples examined in this study were selected from the disordered voice database, model 4337, version 1.03 (Kay Elemetrics Corporation, Lincoln Park, NJ, USA), developed by the Massachusetts Eye and Ear Infirmary Voice and Speech Lab. We included 15 patients with vocal tremor (three males and 12 females, ages 38–81) and 15 normal subjects (four males and 11 females, ages 39–55) from this database. The laryngeal pathologies include paresis, bowing, Parkinson's disease, hyperfunction, vocal fold scarring, vocal fold edema, dyskinesia, and adductor spasmodic dysphonia. Subject information is shown in Table 1, and more detailed subject information is available in the Disordered Voice Database.

The voices were recorded with a sampling rate of $f_s = 44.1$ kHz and 16-bit resolution in a soundproof booth in order to reduce the environment noise. Subjects were asked to sustain the vowel /a/ at a comfortable pitch and intensity, as steadily and as long as possible in order to reduce variances or tremors in the respiratory and articulatory aspects of phonation. In order to avoid transient effects occurring during voice onset and offset, stable segments in the middle of the trial with a length of 1 s were chosen in each sample. These mean that the voice tremors in this study may mainly come from variances in the biomechanical properties of the laryngeal system. We describe the voice segment as $s(t_1)$, $s(t_2)$, $s(t_3)$, …, where $s(t_i) \in \mathbf{R}$, $t_i = iT_s$, $T_s = 1/f_s$, $i = 1, 2, \ldots, N$. Here, N denotes the voice signal length.

Only the sustained vowel /a/ was included in this Disordered Voice Database. Nonlinear dynamic characteristics of other sustained vowels of normal and pathological subjects are also important, and further study might be needed.

2.2. Data analysis

To investigate the nonlinear dynamic characteristics of the tremor voice time series $s(t_i)$, phase space reconstructions and correlation dimensions are employed. Using the time delay technique [28,29], an

Table 1
Subject information

Subject no.	Sex	Age	Diagnosis	Subject no.	Sex	Age	Diagnosis
1	F	52	Normal	16	F	53	Paresis
2	F	43	Normal	17	F	63	Vocal fold bowing
3	M	44	Normal	18	F	54	Adductor spasmodic dysphonia
4	M	44	Normal	19	F	75	Parkinson's Disease
5	F	43	Normal	20	M	76	Hyperfunction
6	F	43	Normal	21	M	69	Vocal fold scarring
7	M	55	Normal	22	F	38	Adductor spasmodic dysphonia
8	F	40	Normal	23	F	49	Vocal fold edema
9	F	43	Normal	24	F	81	Dyskinesia
10	F	45	Normal	25	F	70	Adductor spasmodic dysphonia
11	F	39	Normal	26	F	64	Adductor spasmodic dysphonia
12	F	40	Normal	27	F	38	Hyperfunction
13	M	46	Normal	28	F	73	Adductor spasmodic dysphonia
14	F	39	Normal	29	F	79	Adductor spasmodic dysphonia
15	F	44	Normal	30	M	56	Adductor spasmodic dysphonia

m-dimensional delay-coordinate phase space can be reconstructed as

$$\mathbf{X}_i = \{s(t_i), s(t_i - \tau), \ldots, s(t_i - (m-1)\tau)\}, \tag{1}$$

where m is the embedding dimension and τ the time delay estimated by using the mutual information method [30]. The correlation dimension, D_2, quantifying the dimension of a reconstructed phase space, can be calculated as [31]

$$D_2 = \lim_{r \to 0} \frac{\ln\, C(r)}{\ln(r)} \tag{2}$$

and the improved algorithm proposed by Theiler [32] is used to calculate the correlation integral by

$$C(r) = \frac{2}{(N+1-W)(N-W)} \sum_{n=W}^{N-1} \sum_{i=0}^{N-1-n} \theta\left(r - \left\|\mathbf{X}_i - \mathbf{X}_{i+n}\right\|\right), \tag{3}$$

where r is the radius around $\mathbf{X}_i$, W is set to be the time delay τ, and $\theta(x)$ satisfies

$$\theta(x) = \begin{cases} 1, & x > 0, \\ 0, & x \leqslant 0. \end{cases}$$

In the curve of $\ln C(r)$ versus $\ln(r)$, if the radius r is too small (at the noise level of the signal), random noise will be dominant so that the estimate of D_2 will approach the embedding dimension m and continue to increase with m. If r is too large (about the overall size of the attractor), all dot pairs in the reconstructed phase space will be smaller than r so that the correlation integral will not exhibit scaling behavior and the estimated dimension will be both m and r dependent. Thus, there is a finite region between these two regions, termed the scaling region [31], in which the slopes of the $\ln C(r)$ versus $\ln(r)$ curves increase at first but eventually converge with increasing m. The dimension estimate and its standard deviation were derived using a linear curve fit to the curve of $\ln C(r)$ versus $\ln(r)$ in this scaling region [31–33]. For a sufficiently large embedding dimension m, the estimated dimension is both m and r independent in the scaling region, and a small standard error (less than 5%) of the slope leads to a reliable dimension estimation of a chaotic time series.

Normal voices usually show nearly periodic waveforms and discrete frequency spectra [Fig. 1(a) and (b) of the normal voice from subject 11]. The frequency spectrum of the voice is obtained using the Fourier transform with the Hamming window. During voice production, the vocal folds act as the sound source and radiate sound waves which travel along the vocal tract. The vocal tract modulates these sound waves and outputs a voice signal. Multiple harmonic components can be observed in the amplitude spectrum of the 1 s

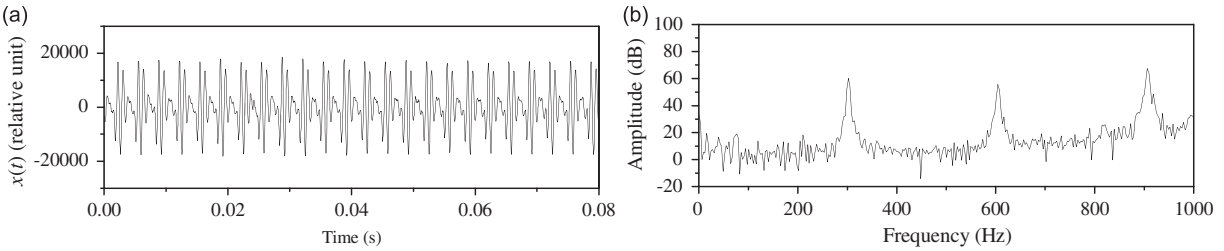

Fig. 1. The nearly periodic waveform (a) and amplitude spectrum (b) of a normal voice from subject 11.

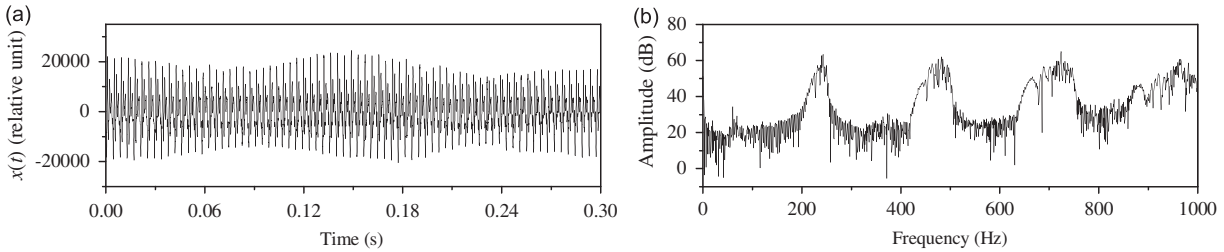

Fig. 2. The low-frequency modulation waveform (a) and amplitude spectrum (b) of a pathological voice from patient 25 with vocal tremor.

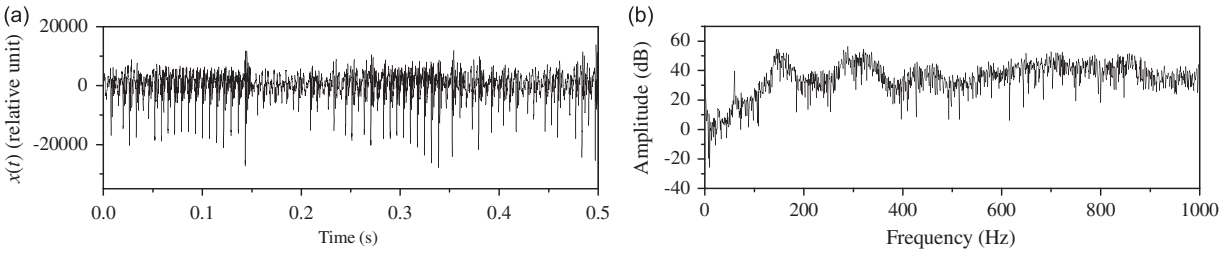

Fig. 3. The aperiodic waveform (a) and broadband amplitude spectrum (b) of a pathological voice from patient 20 with vocal tremor.

voice sample, as shown in Fig. 1(b). In comparison with normal voices, pathological voices from the patients with vocal tremor may display low-frequency modulation and voice irregularities. Fig. 2(a) shows the low-frequency modulation in a tremor voice from subject 25. A series of lateral sideband frequency components around the fundamental frequency can be observed in the amplitude spectrum in Fig. 2(b), where the tremor frequency is estimated to be about 6.7 Hz by calculating the difference between the lateral sideband frequency components and the fundamental frequency. Vocal tremor may also cause a disordered voice with an aperiodic time series and a noise-like broadband spectrum, as shown in Fig. 3(a) and (b) from subject 20. Frequency spectrum analysis qualitatively reveals the different frequency characteristics between the normal and tremor voices. In voice science studies [34,35], voice signals can be classified as type 1, 2, or 3 signals, where type 1 signals are nearly periodic, type 2 signals contain strong frequency modulations or subharmonics, and type 3 signals are irregular and aperiodic. The typical waveforms of these three types of signals are shown in Figs. 1(a), 2(a), and 3(a). Recent studies have found that jitter and shimmer, two traditional perturbation measurements, are appropriate for nearly periodic type 1 signals but may not be applied for type 2 and type 3 signals [34]. Nonlinear dynamic methods, however, provide an important application capable of analyzing all three signal types [35]. Thus, traditional perturbation analysis may be inappropriate for the analysis of the tremor voices used in this study. In order to quantify the low-frequency modulation and irregular tremor voice and determine how many degrees of freedom or variable numbers might be needed for modeling vocal fold

vibrations, nonlinear dynamic analysis, such as correlation dimension analysis, is necessary and will be applied in this study.

Fig. 4(a) shows the correlation integral $\ln C(r)$ versus $\ln(r)$ for the tremor voice in Fig. 3, where the voice sample length is 1 s and the property time delay is $\tau = 16T_s$. The curves from bottom to top correspond to $m = 1,2,\ldots,15$, respectively. In the scaling region ($2^{9.7} < r < 2^{11.8}$), the slope converges to 5.41 ± 0.03 for sufficiently large m. In comparison, we calculated the correlation integrals for the surrogate data of the tremor voice, as shown in Fig. 4(b). The surrogate data are obtained by using the procedure proposed by Theiler [32], i.e., performing a Fourier transform, randomizing the phases of the Fourier components, and then performing an inverse Fourier transform. The surrogate data differs from the tremor voice in that it does not have a scaling region and the slope does not converge with increasing m. The estimated dimension of the tremor voice is significantly less than that of the surrogate data, and thus the results of dimension analysis of the tremor time series can be distinguished from noise data [36,37]. A significant difference between the estimated dimensions for the original and surrogate data can also be found in other tremor voices. This evidence from surrogate analysis further shows that the tremor voices in this study have low-dimensional characteristics. Fig. 4(c) shows the relationship between the estimated dimension and m, in which the curves correspond to the normal voice, the low-frequency modulation tremor voice, the irregular tremor voice, the surrogate data of the irregular tremor voice, and random noise, respectively. As m increases, the estimated dimensions of the random noise and the surrogate data of the irregular tremor voice do not exhibit a saturation tendency;

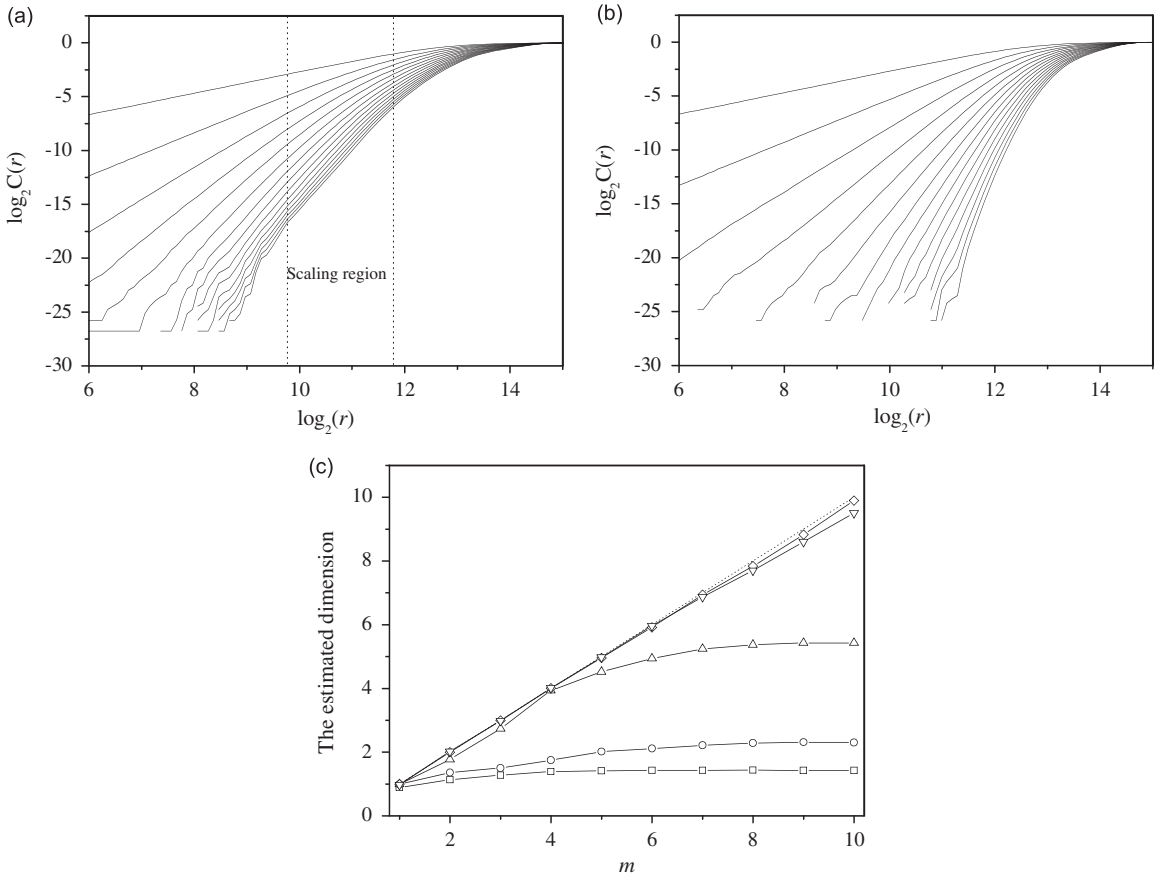

Fig. 4. (a) The correlation integral $\ln C(r)$ versus $\ln(r)$ for the tremor voice, where the curves from bottom to top correspond to $m = 1,2,\ldots,15$ respectively. (b) The correlation integral $\ln C(r)$ versus $\ln(r)$ for the surrogate data of the tremor voice, where the curves from bottom to top correspond to $m = 1,2,\ldots,15$, respectively. (c) The estimated dimension versus m, in which the curves correspond to the normal voice (—□—), the low-frequency modulation tremor voice (—○—), the irregular tremor voice (—△—), the surrogate data of the irregular tremor voice (—▽—), and the random noise (—◇—), respectively.

however, the estimated dimensions of the low-frequency modulation voice and the irregular voice converge to 2.14 ± 0.01 and 5.41 ± 0.03, respectively. This suggests that tremor dynamics are dominated by deterministic nonlinearity.

2.3. Statistical analysis

The correlation dimensions of all the normal and tremor voices are obtained using the above procedure. The Mann–Whitney rank sum test is employed using correlation dimension as the dependent variable and the subject group (normal or tremor) as the independent variable. Statistical analysis is needed to differentiate between normal and tremor groups and a significance level of 0.05 was used. Fig. 5 shows the distributions, D_2, of all normal and tremor voices. The median D_2 values of normal and tremor groups are 1.51 and 3.17, respectively. Statistical analysis using the Mann–Whitney rank sum test reveals that the correlation dimensions of the normal group are significantly lower than those of the tremor group ($p < 0.001$).

In this section, we apply nonlinear dynamic analysis for the voices from patients with vocal tremor. The estimated correlation dimensions of tremor voices converge as the embedding dimension increases, differing from nonconvergent values of its surrogate data and random noise, as shown in Fig. 4(c). This result is significant in that it suggests that tremor voices, like limb tremor [11,12], may have nonlinear dynamic mechanics. All pathological voices from patients with vocal tremor have low-dimensional characteristics, and thus finite state variables may be sufficient to describe the dynamics of voices. During voice production, vocal fold vibrations produce a sound wave traveling in the vocal tract, and then the signal is recorded as voice by using acoustic recording. Because of the physical relevance between vocal fold vibrations and voice signals, it is reasonable to consider that the nonlinear properties of tremor voices are related to the nonlinear features of vocal fold vibrations. A nonlinear model is then necessary to investigate the complex dynamics of vocal tremor. The correlation dimension values of all tremor voices are greater than 2, and thus at least three state variables may be necessary to model the vibrations of the vocal folds with vocal tremor. In addition, as shown in Fig. 5, the correlation dimension values of tremor voices are statistically higher than those of normal voices, which reveal that vocal tremor may be more complex and may require more state variables to describe their dynamics. Therefore, nonlinear dynamic analysis of tremor voices provides valuable information for modeling the vibrations of vocal folds with vocal tremor.

3. Nonlinear model of the vocal folds with vocal tremor

3.1. Vocal tremor model

The tremor voice signals mix vocal fold dynamics with other non-glottal factors, such as vocal tract filtering, aerodynamic noises, and sound radiation, and thus cannot independently monitor the dynamic changes of vocal folds due to vocal tremor. However, in vocal fold models, the system parameters such as tremor

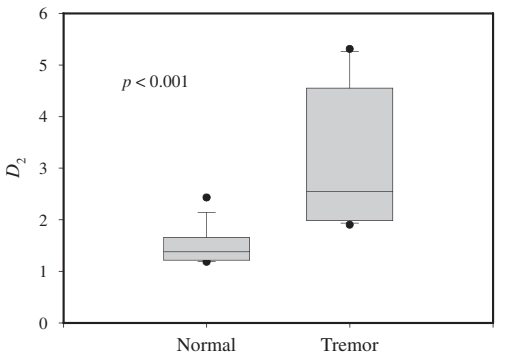

Fig. 5. The distributions, D_2, of all normal and tremor voices, where the line inside the box marks the median, whiskers show 10th and 90th percentiles, and the dots represent outliers.

amplitude, frequency, vocal fold stiffness, and subglottal pressure can be systematically monitored and independently controlled; thus, a vocal fold model can reveal the essential dynamics of a laryngeal system without involving non-glottal factors. In this section, instead of a tremor voice model with other non-glottal factors, we apply a nonlinear vocal fold model to investigate the effect of vocal tremor on vocal fold dynamics. The dynamics of the vocal tremor model will be quantified using nonlinear dynamic methods.

Continuum models allow researchers to simulate vibrations of complex objects [39]. However, numerically solving continuum models for the vocal folds is very time-consuming and complex in computation. It is particularly difficult to study chaotic dynamics of vocal fold vibration coupled with aperiodic glottal airflow using continuum models. In order to quantify chaotic laryngeal activities, simple lumped mass models are still very important. A one-mass model [40] may be an oversimplification of the irregular dynamics of the vocal folds in patients with laryngeal pathologies, since two or more vibratory modes may be needed to capture the vibrations of these pathological vocal folds. Using the above nonlinear dynamic analyses of tremor voices, we have found that at least three state variables may be needed to model vibrations of vocal folds with vocal tremor. The two-mass model [4,25–27] lumps the viscoelastic properties of oscillating vocal fold tissues into mass, stiffness, and damping parameters. It provides a simple yet effective way to capture the primary vibratory features of the vocal folds, and has been successfully used to study the nonlinear vocal fold oscillations in laryngeal pathologies [25–27]. Many interesting phenomena, such as the phase difference between the lower and upper edge of the vocal fold, bifurcation, and chaotic vibration patterns, can be modeled by this concept. However, in most traditional two-mass models, stiffness coefficients are constants and thus cannot be applied to study vocal tremor due to stiffness modulation [4,25–27,41–44]. Previous two-mass models have not investigated the chaotic mechanism of vocal tremor and the effects of tremor amplitude and frequency on vocal fold vibrations. Therefore, in this section, we generalize the two-mass model proposed by Steinecke and Herzel [26] by coupling it with tremor dynamics to investigate the chaotic vibratory characteristics of vocal folds with vocal tremor. This model serves as a simple system to simulate the nonlinear dynamics of vocal fold vibration. More elaborate vocal fold models, such as multiple mass models and finite element models are also important for further study. The systematic diagram of the model of the vocal folds with vocal tremor is shown in Fig. 6. The deduction of the dynamic equation is based on the following conditions:

(1) We focus on investigating the dynamics of vocal fold vibrations, and the interactions [45–47] of the glottal flow with subglottal and supraglottal resonances are neglected. Subglottal pressure, P_s, remains constant and the static component of supraglottal pressure, P_0, is zero [48]. Viscous losses inside the glottis are neglected and the steady glottal airflow satisfies the Bernoulli equation [4,6,25–27,40–44].
(2) The vocal folds are symmetric. The lower and upper parts of each side of the vocal folds can be modeled by a pair of coupled nonlinear oscillators having mass (m), spring constant (k), and damping (r).

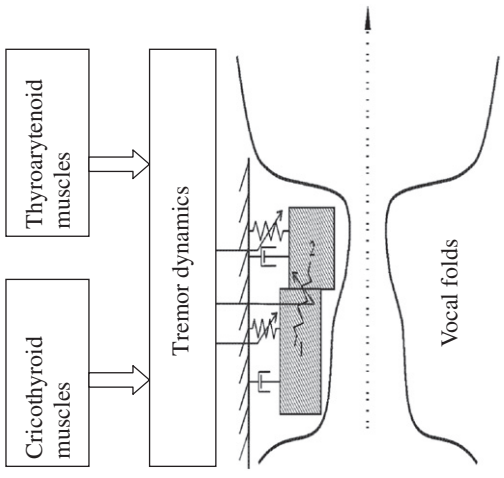

Fig. 6. The systematic diagram of the vocal fold model with vocal tremor dynamics.

(3) The vocal tremor in this study is considered to be from the laryngeal system and the biomechanical stiffness parameters are considered to exhibit rhythmic alterations or low-frequency modulations in pathological vocal tremor. Specifically, slow rhythmic motor unit firings of the thyroarytenoid and the cricothyroid muscles in pathological vocal tremors will produce low-frequency modulations in vocal fold stiffness [14,15,20]. Some non-glottal factors, such as muscle innervation in the diaphragm and vocal tract articulators, may also induce tremor voices. In the model simulation of this study, we focus on vocal tremor in the laryngeal system and describe vocal tremor as a product of abnormal laryngeal muscle innervation. We will not model these non-glottal tremors; however, the principles and methods from nonlinear dynamics can be generalized to the study of non-glottal factors, such as aerodynamic force [44].

For the symmetric vocal folds, two sides of the vocal folds have symmetric dynamics. Considering the above assumptions, we now describe the dynamic equations of the symmetric vocal folds as

$$\begin{aligned} m_1\ddot{x}_1 + r_1\dot{x}_1 + K_1k_1x_1 + \Theta(-a_1)K_1c_1\frac{a_1}{2l} + K_3k_3(x_1 - x_2) &= ld_1P_1, \\ m_2\ddot{x}_2 + r_2\dot{x}_2 + K_2k_2x_2 + \Theta(-a_2)K_2c_2\frac{a_2}{2l} + K_3k_3(x_2 - x_1) &= 0 \end{aligned} \tag{4a}$$

and the vocal tremor dynamics as

$$\dot{K}_i = F_i(K_i) \quad (i = 1, 2, 3), \tag{4b}$$

where x_1 and x_2 are the displacements of the lower (m_1) and upper (m_2) parts of the vocal folds. r_i and k_i denote damping constant and stiffness of the two masses m_i, respectively. Two masses m_1 and m_2 are vertically coupled by a linear spring with the coupling stiffness k_3. During glottal closure, two sides of the vocal folds will collide with each other and produce the restoring force $\Theta(-a_i)K_ic_i(a_i/2l)$ [25,26], where c_i denotes the collision stiffness, d_i is the thickness of mass m_i, and l is the glottis length. The collision function of the vocal folds can be described as [26]

$$\Theta(x) = \begin{cases} \tanh(50x/x_0), & x > 0, \\ 0, & x \leqslant 0. \end{cases} \tag{5}$$

The pressures and glottal volume velocity U from the subglottal region to the minimum glottal diameter satisfy the Bernoulli equation [4,6,25–27,40–44]:

$$P_s = P_1 + \frac{\rho}{2}\left(\frac{U}{a_1}\right)^2 = P_0 + \frac{\rho}{2}\left(\frac{U}{a_{\min}}\right)^2 \text{ and } U = \sqrt{\frac{2P_s}{\rho}}a_{\min}\Theta(a_{\min}) \tag{6}$$

and then the driving pressure P_1 can be deduced as

$$P_1 = P_s\left[1 - \Theta(a_{\min})\left(\frac{a_{\min}}{a_1}\right)^2\right]\Theta(a_1), \tag{7}$$

where

$$a_{\min} = \begin{cases} a_1, & x_1 < x_2, \\ a_2, & x_2 \leqslant x_1, \end{cases}$$

denotes the minimal glottal area, $a_1 = a_0 + 2lx_1$ and $a_2 = a_0 + 2lx_2$ denote the lower and upper glottal areas, respectively, and a_0 is the glottal rest area.

K_i is defined as the stiffness factor described by the tremor dynamics Eq. 4(b). Vocal tremors resulting from laryngeal pathologies may produce low-frequency modulations in the biomechanical parameters of the vocal folds. We thus describe the low-frequency modulation solution of Eq. (4b) as $K_i = F(\omega_T t)$, where $\omega_T/2\pi$ is the tremor fundamental frequency, which is much less than the fundamental frequency $\omega_0/2\pi$ of the vocal fold vibration. The stiffness parameter has been changed unilaterally in previous vocal fold models to study some laryngeal pathologies [26,49]. We thus apply a unified stiffness perturbation factor as $K = K_i$ for all $i = 1, 2, 3$,

and then expand the solution of Eq. (4b) as the following Fourier series:

$$K = C_0 + \sum_{k=1}^{\infty} C_k \sin(k\omega_T t + \theta_k), \tag{8}$$

where C_k is kth coefficient and θ_k is kth phase. For $K = 1$, Eq. (8) can be reduced to the symmetric model of normal vocal folds proposed by Steinecke and Herzel [26] with the default stiffness values given by Ishizaka and Flanagan [25]. In addition, the sinusoidal description $K = C_0 + C_1 \sin(\omega_T t + \theta_1)$ has been applied in previous studies [15,16,20,38], which represent a specific case of Eq. (8) under the first-order expansion. However, this one order expansion is an oversimplification for practical tremor dynamics since tremor voices such as Fig. 2 do not usually show pure sinusoidal patterns. Thus, by combining Eqs. (4) and (8), our model gives a more general description of vocal tremor dynamics.

Considering that the tremor frequency, $\omega_T/2\pi$, is much smaller than the natural frequency of vocal fold vibration, the stiffness perturbation can be described as a quasi-steady process. For sufficiently small damping force, aerodynamic force, and tremor amplitude and frequency, vocal fold collision will not appear, and we thus can approximately solve the displacement x_i by substituting $x_i(t) = x_i(0)\exp(\mathrm{j}\int_0^t \omega\,\mathrm{d}t)$ $(i = 1, 2)$ into Eq. (4a) as

$$x_i(t) = x_i(0)\,\exp\left[\mathrm{j}\int_0^t \omega_0 \sqrt{C_0 + \sum_{k=1}^{\infty} C_k \sin(k\omega_T t + \theta_k)}\,\mathrm{d}t\right] \text{ with } k\omega_T \ll \omega_0, \tag{9}$$

where

$$\omega_0 = \sqrt{\frac{k_1 + k_3}{2m_1} + \frac{k_2 + k_3}{2m_2} \pm \sqrt{\left(\frac{k_1 + k_3}{2m_1} - \frac{k_2 + k_3}{2m_2}\right)^2 + \frac{k_3^2}{m_1 m_2}}}$$

represents the natural frequency of the vocal fold model without vocal tremor. For the band-limited tremor signal ($C_k \ll C_0$), we have the following first approximation solution of Eq. (9):

$$x_i(t) = x_i(0)\,\exp\left[\mathrm{j}\int_0^t \omega_0\sqrt{C_0}\left(1 + \frac{1}{2}\sum_{k=1}^{\infty}\frac{C_k}{C_0}\sin(k\omega_T t + \theta_k)\,\mathrm{d}t\right)\right]. \tag{10}$$

Using the Fourier expansion, Eq. (10) can be expressed as

$$x_i(t) = x_i(0)\,\mathrm{e}^{\mathrm{j}\omega_0\sqrt{C_0}t}\prod_{k=1}^{\infty}\left[\sum_{m=-\infty}^{\infty} j^m J_m(M_k)\,\exp(\mathrm{j}m(k\omega_T t + \theta_k))\right], \tag{11}$$

where $M_k = -(C_k\omega_0/2k\sqrt{C_0}\omega_T)$ and $J_m(\bullet)$ is the m-order Bessel function [50]. Eq. (11) shows that low-frequency vocal tremor can produce a series of side frequencies $\omega_0 \pm m\omega_T$ $(m = 1,2,\ldots)$ around the natural frequency of the vocal folds. Under the assumption of small amplitude, Eq. (11) represents an analytic periodic solution of the tremor model Eqs. (4) and (8). However, for aperiodic vocal fold vibrations, the solution of Eqs. (4) and (8) is difficult to deduce analytically, and numerical calculation is applied. In the following numerical calculations, considering the significant decrease C_k of tremor voices, we apply the two order description of Eq. (8) as $K = C_0 + C_1\sin(\omega_T t) + C_2\sin(2\omega_T t)$. A fourth-order Runge–Kutta method is applied to numerically integrate Eq. (4) with the time step 0.01. Lyapunov exponents are calculated to investigate the global stability of the vocal fold system [41,51], and the Kaplan–Yorke dimension can be obtained using the definition [21]

$$D_L = k + \frac{\sum_{i=1}^{k}\lambda_i}{|\lambda_{k+1}|}, \tag{12}$$

where k satisfies $\sum_{i=1}^{k}\lambda_i \geqslant 0$ and $\sum_{i=1}^{k+1}\lambda_i < 0$. Based on the measurements of vocal fold tissue properties, Ishizaka and Flanagan [25] gave default values of the biomechanical parameters of the two-mass vocal fold model. The parameter values are listed in Table 2. Here, the used subglottal pressure level of 15 cm H_2O is within the pressure range given by Ishizaka and Flanagan [25]. The tremor frequency and amplitude can be

Table 2
Parameter values for the vocal fold model

	Model parameters
m_1	0.125
m_2	0.025
r_1	0.01
r_2	0.01
k_1	0.08
k_2	0.008
c_1	$3k_1$
c_2	$3k_2$
k_3	0.025
d_1	0.25
d_2	0.05
a_0	0.1
P_s	0.015
l	1.4
ρ	0.00113

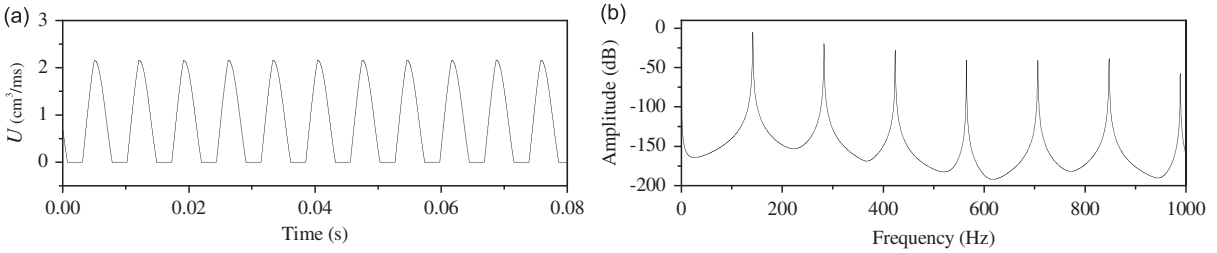

Fig. 7. The periodic time series (a) and amplitude spectrum (b) of the glottal volume velocity U of the model.

obtained based on previous voice analysis [13–15,20]. Our recent studies in vocal fold modeling and excised larynx experiments have shown that extremely high subglottal pressure may produce chaotic laryngeal activities [41,51], while the applied $P_s = 0.015$ in this study is not high enough to induce chaotic vocal fold vibrations for the above system parameter set. All parameters are given in units of cm, g, ms and their corresponding combinations.

3.2. Low-frequency modulation and chaotic vibration of the vocal tremor model

For $K = 1$ of the normal vocal folds, Fig. 7(a) and (b) show the periodic time series of the glottal area signal U with length 1 s and discrete frequency spectrum, respectively. The zero glottal volume flow velocity, U, is associated with vocal fold collision. The Lyapunov exponents are calculated as $\lambda_1 \approx 0$, $\lambda_2 \approx -0.144$, $\lambda_3 \approx -0.168$, and $\lambda_4 \approx -0.168$, and the Kaplan–Yorke dimension $D_L = 1$ can be obtained. By calculating the Fourier transform of the displacement signal x_1, we can use spectrum analysis to extract the side frequency due to vocal tremor around the fundamental frequency of vocal fold vibrations. For the tremor dynamics $K = C_0 + C_1 \sin(\omega_T t) + C_2 \sin(2\omega_T t)$ with $C_0 = 1$, $C_1 = 0.2$, $C_2 = 0$, and $\omega_T/2\pi = 5$ Hz, Fig. 8(a) shows the low-frequency modulation of the waveform that can be theoretically described by Eq. (11). The small amplitude approximation of Eq. (11) is effective in revealing the physical mechanism of vocal tremor. Based on previous tremor voice analysis [13–15,20], we use the relative tremor amplitude of $C_1/C_0 = 0.2$ and the tremor frequency $\omega_T/2\pi = 5$ Hz. The corresponding amplitude spectrum in Fig. 8(b) shows a series of side frequencies around the natural frequency of the vocal folds. Rewriting Eq. (8) into an autonomous form by adding the variable $z = \omega_T t$, we can obtain the Lyapunov exponents as $\lambda_1 \approx 0$, $\lambda_2 \approx 0$, $\lambda_3 \approx -0.148$, $\lambda_4 \approx -0.166$, and $\lambda_5 \approx -0.166$, and the Kaplan–Yorke dimension as $D_L = 2$. Thus, the low-frequency tremor modulation

gives a quasi-periodic solution of the vocal fold system. Furthermore, for the vocal tremor dynamics with $C_0 = 1$, $C_1 = 0.3$, $C_2 = 0.6$, and $a_0 = 0.025$, an aperiodic time series can be observed in Fig. 9(a), and a broadband amplitude spectrum is shown in Fig. 9(b). The Lyapunov exponents are calculated as $\lambda_1 \approx 0.058$, $\lambda_2 \approx 0$, $\lambda_3 \approx 0$, $\lambda_4 \approx -0.096$, and $\lambda_5 \approx -0.442$, respectively. The Kaplan–Yorke dimension $D_L \approx 3.6$. The positive Lyapunov exponent and fractal dimension demonstrate evidence of chaos in vocal fold systems with vocal tremor.

The two-mass model of the vocal folds with vocal tremor can produce periodic, quasi-periodic, and chaotic behaviors that are also observed in the tremor voice analysis from Figs. 1 to 3. It should be noted that the vocal fold model of Eq. (4) cannot give completely consistent simulations for the real tremor voices, since some non-glottal factors, such as the vocal tract, have not been included in this vocal fold model and the model parameters of the real voice have not been predefined. Modeling tremor voices involves the interaction among the vocal folds, subglottal tract, and supraglottal tract, which requires further study. However, this vocal fold model effectively reveals the dynamic mechanism of aperiodic vocal fold vibration due to vocal tremor and predicts how the vocal tremor parameters of amplitude and frequency affect vocal fold dynamics.

Although chaotic vocal fold vibration has been reported in our previous studies [27,41,44], the dynamics of vocal folds with vocal tremor has not yet been studied in general laryngeal diseases and a general vocal tremor model has not been proposed. A specific case of vocal tremor has been reported in Parkinson's disease [16]. However, nonlinear dynamic analysis was not used in that study, and the nonlinear dynamic mechanism of tremor voices was not investigated. Furthermore, the study used a high stiffness coefficient, which is not the case in most laryngeal diseases. Different laryngeal diseases have different pathophysiological mechanisms causing varying changes of vocal fold stiffness. Thus, the model with high vocal fold stiffness in Ref. [16] cannot study the tremor dynamics of general laryngeal diseases. Our study further shows that in addition to a high stiffness coefficient [16], periodic stiffness perturbation may also induce chaotic vibrations in vocal fold systems. Chaotic vibration has a higher dimension value than periodic vibration, as observed in Fig. 4(c). Unlike the single sinusoidal modulation of the Parkinsonian vocal model in Ref. [16], this study provides a more general model described by Eqs. (4b) and (8) to describe vocal tremors in different laryngeal diseases. In the experimental study, a number of voice samples from laryngeal diseases such as paresis, hyperfunction, scarring, Parkinson's disease, and adductor spasmodic dysphonia were applied. By employing nonlinear dynamic analysis on these tremor voices, the nonlinear dynamic mechanism was revealed. This study shows

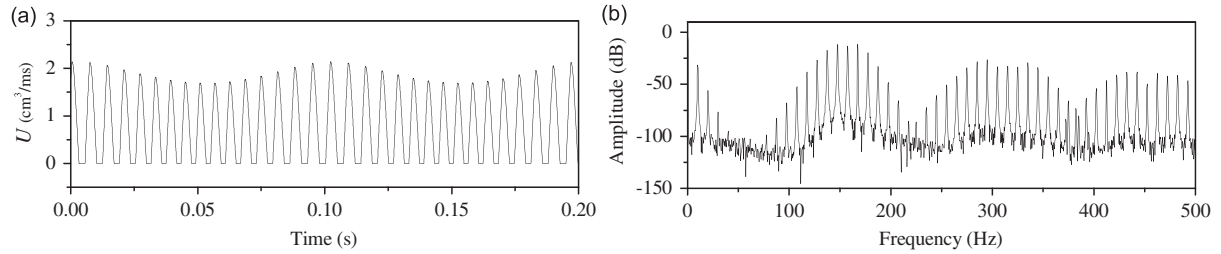

Fig. 8. The low-frequency modulation time series (a) and amplitude spectrum (b) of the glottal volume velocity U of the model, where $C_0 = 1$, $C_1 = 0.5$, and $\omega_T/2\pi = 5$ Hz.

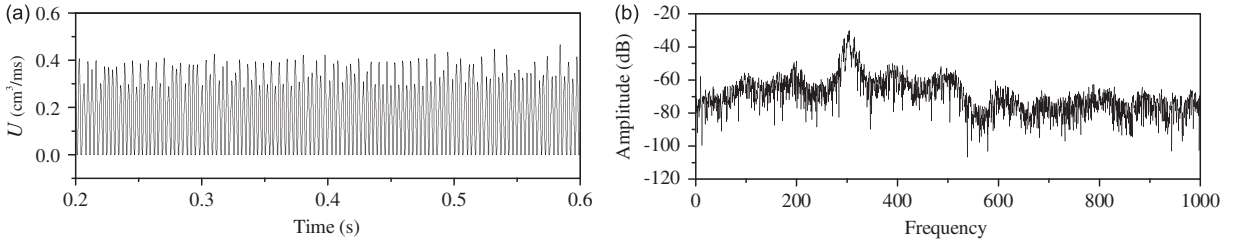

Fig. 9. The aperiodic time series (a) and broadband amplitude spectrum (b) of the glottal volume velocity U of the model, where $C_0 = 4$, $C_1 = 0.6$, $a_0 = 0.025$, and $\omega_T/2\pi = 5$ Hz.

that vocal tremor represents a general phenomenon and can be widely found in laryngeal diseases. This study of the dynamic mechanism of vocal tremor may have clinical and scientific value for the understanding of vocal tremor dynamics in general laryngeal pathologies.

3.3. Effects of tremor amplitude and frequency

To show the effect of tremor amplitude, the bifurcation diagrams with and without vocal tremor are given in Figs. 10(a) and 11(a), respectively, where the velocity $v_1 = \dot{x}_1$, obtained from the Poincare section at $x_1 = 0$ versus the stiffness coefficient k_3, are illustrated. The corresponding Lyapunov exponents are given in Figs. 10(b) and 11(b). For the vocal folds without vocal tremor, high periodic vibrations and fine period-doubling bifurcation can be observed in the bifurcation diagrams with increasing k_3, where periodic and chaotic vibrations are represented by the discrete and scattered points, respectively. The bifurcation points are located at $\lambda_2 \approx 0$ in Fig. 10(b), and the regions of chaotic vibration can be found at $\lambda_1 > 0$. However, for the vocal tremor dynamics $K = C_0 + C_1 \sin(\omega_T t) + C_2 \sin(2\omega_T t)$ with $C_1 = 0.03$ and $C_2 = 0.5C_1$, the periodic stiffness perturbation will drive the trajectories from the basins of periodic attractors to nearby chaotic attractors, and thus there is no significant difference between their positive Lyapunov exponents. Low-frequency stiffness perturbation smears out the fine bifurcation structures, inhibits the period-doubling bifurcation cascade, and broadens the intervals of chaotic vibrations in the bifurcation diagram (Fig. 11). Thus, the vocal folds with vocal tremor show a broader chaotic region than the vocal folds without vocal tremor. The fact that only a few period-doubling bifurcations can be found in tremor voice data may be related to clinical observation. In contrast, infinite period-doubling bifurcation cascades can be found in the deterministic vocal fold system without vocal tremor.

In Fig. 12, the contour plane shows the grey-coded value of the maximal Lyapunov exponent λ_1 with respect to the tremor amplitude C_1 and frequency $\omega_T/2\pi$, where $C_2 = 0.5C_1$, $k_1 = 0.044$, and the black and white regions correspond to $\lambda_1 > 0$ and $\lambda_1 \approx 0$, respectively. For sufficiently large tremor amplitude, chaotic vibrations with positive Lyapunov exponents can be seen. When the system stiffness parameters are perturbed,

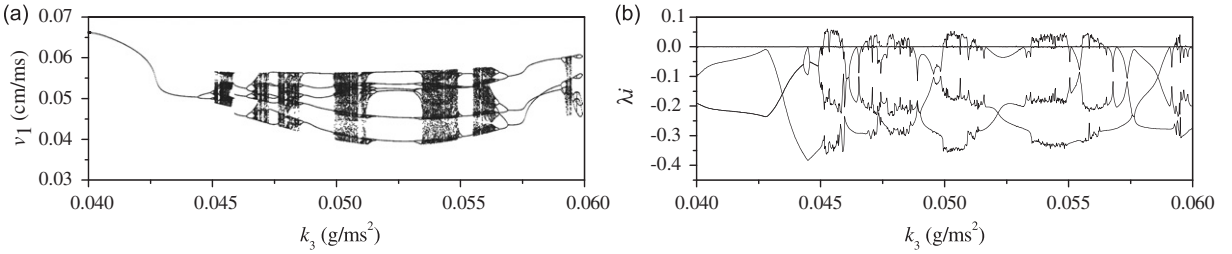

Fig. 10. The vocal-fold model without vocal tremor: (a) bifurcation diagrams, where the Poincare sections $v_1 = \dot{x}_1$ at $x_1 = 0$ versus the coupling stiffness coefficient k_3 are illustrated. (b) Lyapunov exponents λ_i versus k_3, where the curves from top to bottom correspond to λ_1, λ_2, λ_3, and λ_4, respectively.

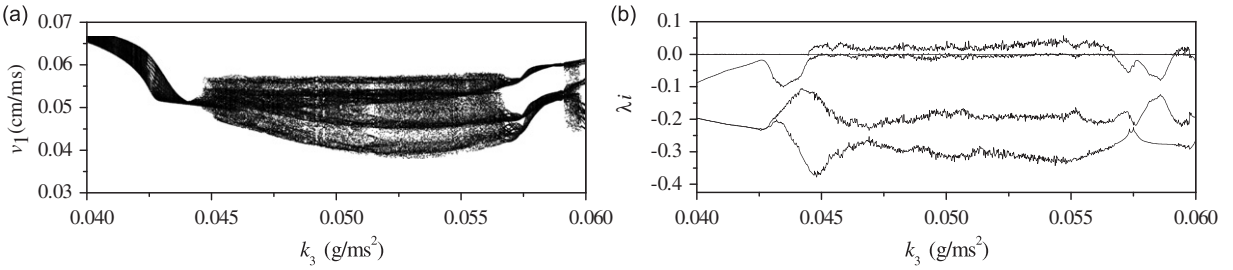

Fig. 11. The vocal fold model with vocal tremor, where $C_1 = 0.03$: (a) bifurcation diagrams, where the Poincare sections v_1 at $x_1 = 0$ versus the coupling stiffness coefficient k_3 are illustrated. (b) Lyapunov exponents λ_i versus k_3, where the curves from the top correspond to λ_1, λ_2, λ_3, λ_4, and λ_5, respectively.

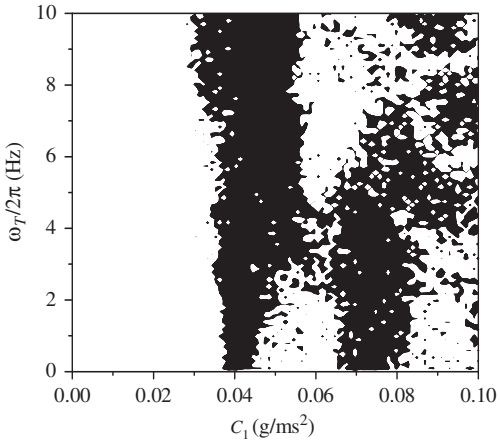

Fig. 12. The grey-coded value of the maximal Lyapunov exponent λ_1 with respect to the tremor amplitude C_1 and frequency $\omega_T/2\pi$, where the black and white regions correspond to $\lambda_1 > 0$ and $\lambda_1 \approx 0$, respectively.

system dynamic behaviors will change correspondingly. With sufficiently large tremor amplitude, the trajectory will be driven to a nearby chaotic attractor, and chaotic regions in the bifurcation diagram will broaden. Similar phenomena have been observed in our previous model study [44], where turbulent noise generated by unsteady glottal airflow was applied as an external aerodynamic perturbation factor. Thus, biomechanical perturbation factors may increase the vibratory complexity of the vocal folds.

4. Conclusion

In this paper, we have studied nonlinear dynamic characteristics of vocal tremor using voice analysis and model simulation. Low-frequency modulation and aperiodicity have been found in tremor voices. The tremor voices from patients with laryngeal diseases, such as paresis, Parkinson's disease, hyperfunction, and adductor spasmodic dysphonia showed low-dimensional characteristics, differing from random noise. The correlation dimensions of tremor voices were statistically higher than normal voices. Furthermore, based on the results of nonlinear dynamic analysis of tremor voice, a nonlinear vocal tremor model was proposed. Under small amplitude approximation, the analytic solution of the model was expanded as a series of Bessel functions. For aperiodic vocal fold vibrations, fractal dimension and positive Lyapunov exponents showed evidence of chaos. Tremor amplitude and frequency represent important parameters in governing vocal fold dynamics. Sufficiently large tremor amplitude may cause chaotic vocal fold vibrations. The results from voice analysis and model simulation revealed the nonlinear dynamic mechanism of vocal tremor. Vocal tremor can be found in patients with laryngeal disorders, and thus nonlinear dynamic analysis and modeling of vocal tremor may be helpful for understanding the dynamic mechanisms of laryngeal disorders and may be valuable for developing new methods for early diagnosis of laryngeal diseases and evaluation of clinical treatment.

Acknowledgment

This study was supported by NIH Grant no. 1-R01DC05522-01 from the National Institute of Deafness and other Communication Disorders.

References

[1] S.R. Bishop, M.J. Clifford, Zones of chaotic behavior in the parametrically excited pendulum, *Journal of Sound and Vibration* 189 (1996) 142–147.

[2] Y. Zhang, G.H. Du, Spatio-temporal synchronization of coupled parametrically excited pendulum arrays, *Journal of Sound and Vibration* 239 (2001) 983–994.

[3] S. Bowong, F.M. Moukam Kakmeni, J.L. Dimi, Chaos control in the uncertain Duffing oscillator, *Journal of Sound and Vibration* 292 (2006) 869–880.
[4] J.C. Lucero, Oscillation hysteresis in a two-mass model of the vocal folds, *Journal of Sound and Vibration* 282 (2005) 1247–1254.
[5] C.E. Vilain, X. Pelorson, C. Fraysse, M. Deverge, A. Hirschberg, J. Willems, Experimental validation of a quasi-steady theory for the flow through the glottis, *Journal of Sound and Vibration* 276 (2004) 475–490.
[6] I.R. Titze, R. Baken, H. Herzel, Evidence of chaos in vocal fold vibration, in: I.R. Titze (Ed.), *Vocal Fold Physiology: New Frontier in Basic Science*, Singular, San Diego, 1993, pp. 143–188.
[7] A. Facchini, C.V. Bellieni, N. Marchettini, F.M. Pulselli, E.B.P. Tiezzi, Relating pain intensity of newborns to onset of nonlinear phenomena in cry recordings, *Physics Letters* A338 (2005) 327–332.
[8] A. Beuter, K. Vasilakos, Tremor: is Parkinson's disease a dynamical disease?, *Chaos* 5 (1995) 35–42.
[9] A. Blitzer, M.F. Brin, C.T. Sasaki, S. Fahn, K.S. Harris, *Neurologic Disorders of the Larynx*, Thieme, New York, 1992.
[10] L.J. Findley, W.C. Koller, Essential tremor: a review, *Neurology* 37 (1987) 1194–1197.
[11] M.S. Titcombe, L. Glass, D. Guehl, A. Beuter, Dynamics of Parkinsonian tremor during deep brain stimulation, *Chaos* 11 (2001) 766–773.
[12] N. Sapir, R. Karasik, S. Havlin, E. Simon, J.M. Hausdorff, Detecting scaling in the period dynamics of multimodal signals: application to Parkinsonian tremor, *Physical Review* E67 (2003) 031903.
[13] E.W. Massey, G.W. Paulson, Essential vocal tremor: clinical characteristics and response to therapy, *Southern Medical Journal* 78 (1985) 316–317.
[14] D.G. Hanson, B.R. Gerratt, P.H. Ward, Cinegraphic observations of laryngeal function in Parkinson's disease, *Laryngoscope* 94 (1984) 348–353.
[15] M. Gresty, D. Buckwell, Spectral analysis of tremor: understanding the results, *Journal of Neurology, Neurosurgery, and Psychiatry* 53 (1990) 976–981.
[16] Y. Zhang, J.J. Jiang, D.A. Rahn, Studying vocal fold vibrations in Parkinson's disease with a nonlinear model, *Chaos* 15 (2005) 033903.
[17] I.R. Titze, Coupling of neural and mechanical oscillators in control of pitch, vibrato, and tremor, in: P. Davis, N. Flecher (Eds.), *Vocal Fold Physiology: Controlling Complexity and Chaos*, Singular, San Diego, 1996, pp. 47–62.
[18] H. Ackermann, W. Ziegler, Cerebellar voice tremor: an acoustic analysis, *Journal of Neurology, Neurosurgery, and Psychiatry* 54 (1991) 74–76.
[19] D.E. Hartman, B. Vishwanat, Spastic dysphonia and. essential (voice) tremor treated with primidone, *Archives of Otolaryngology* 110 (2003) 394–397.
[20] W.S. Winholtz, L.O. Ramig, Vocal tremor analysis with the vocal demodulator, *Journal of Speech, Language, and Hearing Research* 35 (1992) 562–573.
[21] E. Ott, T. Sauer, J.A. Yorke, *Coping With Chaos: Analysis of Chaotic Data and the Exploitation of Chaotic Systems*, Wiley, New York, 1994.
[22] I. Hertrich, W. Lutzenberger, S. Spieker, H. Ackermann, Fractal dimension of sustained vowel productions in neurological dysphonias: an acoustic and electroglottographic analysis, *Journal of the Acoustical Society of America* 102 (1997) 652–654.
[23] Y. Zhang, C. McGilligan, L. Zhou, M. Vig, J.J. Jiang, Nonlinear dynamic analysis of voices before and after surgical excision of vocal polyps, *Journal of the Acoustical Society of America* 115 (2004) 2270–2277.
[24] A. Giovanni, M. Ouaknine, J.-M. Triglia, Determination of largest Lyapunov exponents of vocal signal: application to unilateral laryngeal paralysis, *Journal of Voice* 13 (1998) 341–354.
[25] K. Ishizaka, J.L. Flanagan, Synthesis of voiced sounds from a two-mass of the vocal cords, *Bell System Technical Journal* 51 (1972) 1233–1268.
[26] I. Steinecke, H. Herzel, Bifurcations in an asymmetric vocal-fold model, *Journal of the Acoustical Society of America* 97 (1995) 1874–1884.
[27] Y. Zhang, J.J. Jiang, Chaotic vibratory behaviors of the vocal-fold model with a unilateral polyp, *Journal of the Acoustical Society of America* 115 (2004) 1266–1269.
[28] N.H. Packard, J.P. Crutchfield, J.D. Farmer, R.S. Shaw, Geometry from a time series, *Physical Review Letters* 45 (1980) 712–715.
[29] F. Takens, Detecting strange attractors in turbulence, in: D.A. Rand, B.S. Young (Eds.), *Lecture Notes in Mathematics*, 898, Springer, Berlin, 1981, pp. 366–381.
[30] A.M. Fraser, H.L. Swinney, Independent coordinator for strange attractors from mutual information, *Physical Review A* 33 (1986) 1134–1240.
[31] P. Grassberger, I. Procaccia, Measuring the strangeness of strange attractors, *Physica D* 9 (1983) 189–208.
[32] J. Theiler, Spurious dimension from correlation algorithm applied to limited time-series data, *Physical Review A* 34 (1986) 2427–2432.
[33] P.E. Rapp, T.A.A. Watanabe, P. Faure, C.J. Cellucci, Nonlinear signal classification, *International Journal of Bifurcation and Chaos* 2 (2006) 1273–1293.
[34] I.R. Titze, Workshop on Acoustic Voice Analysis: Summary Statement, National Center for Voice and Speech, Denver, CO, 1995, p. 36.
[35] Y. Zhang, J.J. Jiang, Nonlinear dynamic analysis of signal typing of pathological human voices, *Electronics Letters* 39 (2003) 1021–1023.
[36] J. Theiler, S. Eubank, A. Longtin, B. Galdrikian, J.D. Farmer, Testing for nonlinearity in time series: the method of surrogate data, *Physica D* 58 (1992) 77–94.

[37] A. Jedynak, M. Bach, J. Timmer, Failure of dimension analysis in a simple five-dimensional system, *Physical Review E* 50 (1994) 1770–1780.
[38] R. Laje, T. Gardner, G.B. Mindlin, Neuromuscular control of vocalization in bird song: a model, *Physical Review E* 65 (2002) 051921.
[39] J.J. Jiang, C.E. Diaz, D.G. Hanson, Finite element modeling of vocal fold vibration in normal phonation and hyperfunctional dysphonia: implications for the pathogenesis of vocal nodules, *Annals of Otology, Rhinology, and Laryngology* 107 (1998) 603–610.
[40] J. Flanagan, L. Landgraf, Self-oscillating source for vocal-tract synthesizers, *IEEE Transactions on Audio and Electroacoustics* 16 (1968) 57–64.
[41] J.J. Jiang, Y. Zhang, J. Stern, Modeling of chaotic vibrations in symmetric vocal folds, *Journal of the Acoustical Society of America* 110 (2001) 2120–2128.
[42] B.H. Story, I.R. Titze, Voice simulation with a body-cover model of the vocal folds, *Journal of the Acoustical Society of America* 97 (1995) 1249–1260.
[43] I.R. Titze, B.H. Story, Rules for controlling low-dimensional vocal fold models with muscle activation, *Journal of the Acoustical Society of America* 112 (2002) 1064–1076.
[44] J.J. Jiang, Y. Zhang, Chaotic vibration induced by turbulent noise in a two-mass model of vocal folds, *Journal of the Acoustical Society of America* 112 (2002) 2127–2133.
[45] S.F. Austin, I.R. Titze, The effect of subglottal resonance upon vocal fold vibration, *Journal of Voice* 11 (1997) 391–402.
[46] Z. Zhang, J. Neubauer, D.A. Berry, The influence of subglottal acoustics on laboratory models of phonation, *Journal of the Acoustical Society of America* 120 (2006) 1558–1569.
[47] Z. Zhang, J. Neubauer, D.A. Berry, Aerodynamically and acoustically driven modes of vibration in a physical model of the vocal folds, *Journal of the Acoustical Society of America* 120 (2006) 2841–2849.
[48] T. Baer, Investigation of the phonatory mechanism, *ASHA Report* 11 (1981) 38–47.
[49] T. Wurzbacher, R. Schwarz, M. Döllinger, U. Hoppe, U. Eysholdt, J. Lohscheller, Model-based classification of nonstationary vocal fold vibrations, *Journal of the Acoustical Society of America* 120 (2006) 1012–1027.
[50] N.W. McLachlan, *Bessel Functions for Engineers*, Oxford University Press, London, 1955.
[51] J.J. Jiang, Y. Zhang, C.N. Ford, Nonlinear dynamics of phonations in excised larynx experiments, *Journal of the Acoustical Society of America* 114 (2003) 2198–2205.